On the relevance of the light of the night sky (LONS) in the photosensor choice for the next generation of Cherenkov telescopes

M. Dosil, M. Martinez
IFAE, Barcelona, Spain

Abstract: The interplay between variables like the actual expected number of photons per cell due to the diffuse component of the light of the night sky (LONS), the photosensor gain and quantum efficiency, the electronics noise and time response, the first level trigger scheme and the acceptable trigger rate (among others) when trying to lower as much as possible the threshold in an Imaging Air Cherenkov Telescope, are discussed in detail. Numerical estimates produced with detailed simulations for three types of photosensors being considered for the next generation of telescopes (PMTs, HPDs and APDs) are presented and compared.

1. Introduction

One of the main aims of the next generation of Imaging Air Cherenkov Telescopes is reaching the lowest possible gamma ray energy threshold. A threshold goal of gamma energies below 10 GeV is part of the “raison d’être” of telescopes such a MAGIC [1] and has a very important impact in the expected physics program. For this purpose, their design foresees the use of a large mirror (17 m diameter for MAGIC) and the use of very sensitive photosensors for the camera cells.

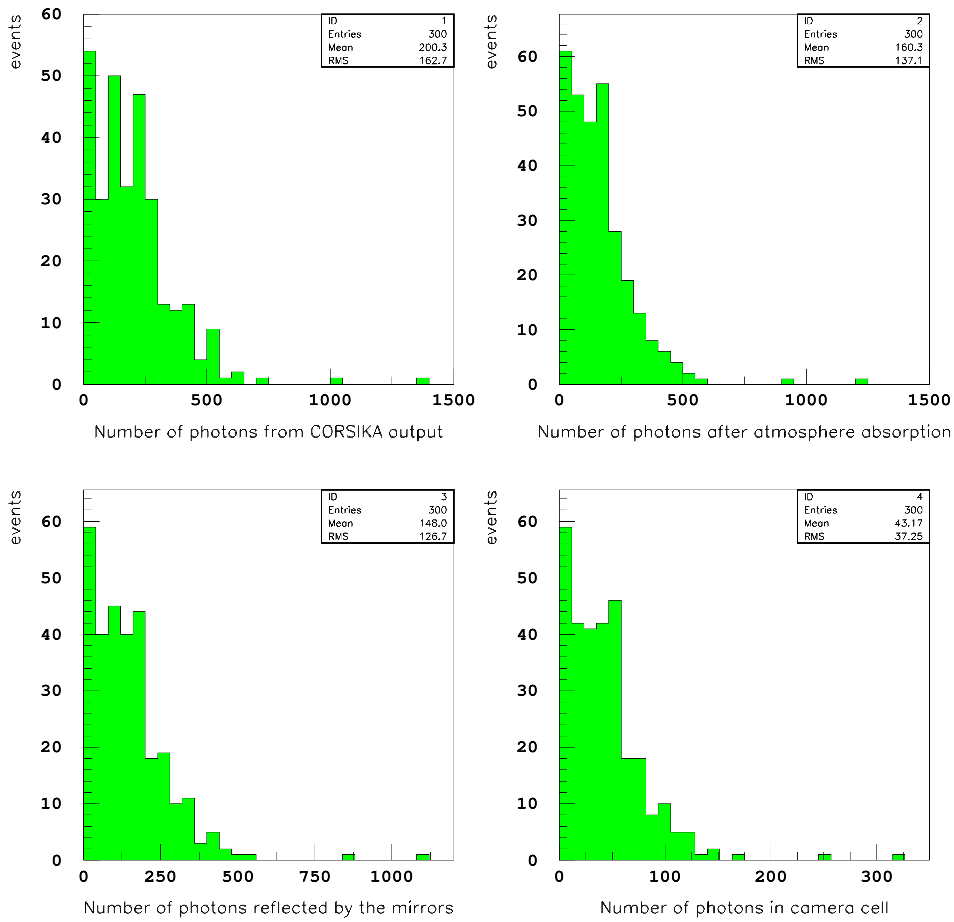

Figure 1: Light distribution of 10 GeV gamma showers generated at zero zenith and 50 m impact parameter. The last plot is the expected number of photons in the most illuminated camera cell of each event.

Nevertheless, just to get a feeling on the demanding such a low threshold goal is, figure 1 shows the distribution of the expected number of photons coming from a 10 GeV gamma shower at different stages[1]. The average expected number of photons in the camera cell with higher illumination is of about 43. Taking into accounts the camera cell signal losses (light losses in the Winston cone, photosensor quantum and collection efficiencies) one might expect a rather low final number of signal photoelectrons in the camera cells (for instance below 10 photoelectrons for good photomultipliers).

[1] For all the studies described in this note, the actual design parameters of the MAGIC telescope [1] have been used.

Current IACTs use photomultipliers (PMTs) as photosensors. PMTs have a very large gain and small electronic noise but, on the other hand, have limited quantum efficiency (about 12 percent in the relevant region for Cherenkov telescopes), non-negligible excess noise factors (above $ENF=1.20$) and important afterpulsing effects.

Two other alternatives are being explored for an improved sensitivity: avalanche photodiodes (APDs) and hybrid photodetectors (HPDs) see reference [1].

- The main advantage of the APDs is their very high quantum efficiency ($QE > 70$ %) over the whole interesting wavelength range, which should allow to reduce the trigger threshold of the telescope and improve the image reconstruction efficiency just above threshold. Their main limitation is the noise, both its intrinsic high amplification noise, which for high-enough gains can hardly be driven below $ENF=2$, and the detector-capacitance term of the electronic noise for the unavoidably needed preamplifier system. In another note [2] we've discussed already these limitations in quite detail.

- The main advantage of the HPDs with a GaAsP photocatode is their relatively high quantum efficiency ($QE > 40$ %) together with their ability to resolve single photoelectrons due to an intrinsic high gain $O(10^4)$ and a negligible excess noise factor ($ENF<1.05$). In the MAGIC case, in which observations at large zenith angles and in the presence of moonlight are foreseen and, hence, red-sensitive photodetectors are needed, one of the limitations of present HPDs is their limited quantum efficiency in the red, which can be overcome by using the proper wavelength-shifter coating. Another relevant limitation at present is their high prize, linked to the complex procedure needed to produce them but mostly due to the monopoly of just one company producing them.

  In order to estimate which of these alternatives would allow a lower threshold, a straight argumentation would conclude that the devices with larger quantum efficiency should be the best. Since with higher quantum efficiency the photostatistics is higher, that should allow a direct decrease of the trigger threshold.

  In practice, however, other considerations do play an important role in spotting the best device to decrease the threshold, since on top of the relevant signal, there will always be different noise sources which have to be taken into account:

- The device amplification noise quantified by the Excess Noise Factor.

- The electronic noise of the device and its preamplification electronics (if needed).

- The pileup noise due to the finite time response of the whole pixel chain.

- The photonic noise due to the Light of the Night Sky.

The importance of having a small Excess Noise Factor to allow an absolute photodetector calibration and, hence, a precise trigger threshold setting was already discussed in reference [2]. The electronic noise can usually be diminished by using long-enough pulse-shaping times but, unfortunately, that increases the last two noise sources since that means having larger probability of pulse pileup and also integrating more Light of the Night Sky background. The increase of that last noise may, in turn, require an increase in the pixel threshold to have a manageable trigger rate.

Given the fact that, for the devices described above, not only the Quantum Efficiencies are different but also the time response and noise characteristics are different, a reliable evaluation of the lower threshold attainable with each one requires a detailed study of the interplay of these variables.

In order to do that, we've performed a realistic simulation of the camera trigger rate under the known characteristics of the photosensors scrutinized and the measured level of the Light of the Night Sky. To understand the effect of the different characteristics, the simulation has been performed in two steps:

1. In the first one, the evaluation has been performed neglecting the pixel noises (electronic noise and ENF)

2. In the second, all the known sources of pixel noise have been properly taken into account.

In this note we discuss first the meaning and magnitude of the Night-Sky Background (NSB). Afterwards, the actual technique used to generate the diffuse NSB events is presented and the expected trigger rates computed. Then, with a couple of different techniques, the results are extrapolated to obtain the threshold setting needed to keep a trigger rate as low as 10 Hz. Also a clue on the analysis variables which shall allow to discriminate the NSB events against the gamma ray events is presented. Finally, the results when the pixel noises are taken into account are presented.

2. The night-sky background.

Night-sky background (NSB) is one of the most important factors in limiting the energy threshold of atmospheric Cherenkov telescopes. Two kinds of NSB can be distinguished [1]:

- Diffuse NSB.
  This night-sky background is also named LONS (light of the night sky) and it sums up the light coming from several sources: the air fluorescence, the starlight of faint stars ($m \geq 10$) and also the light due to air glow. Eventually, depending on the site, part of this diffuse NSB is due to the man-made artificial light.

- NSB due to starlight.
  Bright stars in the field-of-view of the camera can disturb the observation of an object. By knowing the light distribution of the star field we can remove this light in the on-line or off-line trigger level.

The NSB will cause accidental triggers and will also contaminate the gamma images close to the energy threshold. It will also affect the angular acceptance, the light collection area, the time response and the spectral sensitivity of our telescope.

The intensity of the diffuse NSB was measured at the site of the "El Roque de los Muchachos" observatory on the Canary Island of "La Palma" [3], which provides one of the best sky in the world for astronomical observations. This measurement was performed using the single photo-electron counting technique in the wavelength range of 300-600 nm for the wide angle integrating and narrow angle detectors. This spectral range was chosen since the PMT with bialkali photocathode (widely used in ground based Cherenkov detectors) are sensitive to light in the range of 300 to 600 nm.

We use here the result for a narrow angle detector (angular acceptance ≤ 1 degree) since this will be the case of the finely pixelized future Cherenkov telescopes. This means that the detector integrates the starlight due to faint stars in a small solid angle. Therefore, according to this measurement, we took for our studies the NSB photon flux to be:

$$\phi = (1.75 \pm 0.4) \cdot 10^{12} \ \mathrm{ph} / \mathrm{m}^2 \cdot sr \cdot s \qquad (1)$$

If we take into account specifically the MAGIC characteristics, namely, 236 m^2 of mirror area, 0.05^0 pixel radius and 90% mirror reflectivity we get the following photon rate:

$$\text{photon rate} = 0.9 \ \mathrm{photons} / \mathrm{nsec} \qquad (2)$$

3. Generation of diffuse NSB events in the MAGIC camera Monte Carlo.

We assume that we can characterize the diffuse NSB events with a Poisson distribution. Therefore, we generated Poisson randomly distributed events in the camera plane for the 3 types of photodetectors being considered, namely PMT, HPD, and APD, and for 5nsec and 10nsec integration times. We also took the NSB photon rate given in the expression (2). We summarize in the following table the characteristics of the events generated.

Photo-detector	**Quantum Efficiency (%)[1]**	**Integration time (nsec)**	**<number of photoelectrons>**
PMT	12	5	0.5
HPD	45	5	2.0
APD	80	5	3.6
PMT	12	10	1.1
HPD	45	10	4.0
APD	80	10	7.2

Table1: Characterization of the events generated.

[1] Average quantum efficiency for the 300 – 600 nm wavelength range.

Assuming that the trigger region consists of 127 pixels of 0.1^0 diameter each. The trigger condition used in our simulation program [4] was *at least 4 neighbor close-packed pixels above a certain photoelectron threshold N inside the trigger region*. That is, we implement the *4NN* trigger condition.

Therefore, the probability that a pixel has N photoelectrons or more is given by the cumulative Poisson probability, namely:

$$P(x \geq N) = 1 - \sum_{k=0}^{N-1} \frac{e^{-\mu} \cdot \mu^{x}}{K!} \qquad (3)$$

where x is the number of photoelectrons of the pixel and μ is the mean number of photoelectrons which depends on the photodetector and integration time (see Table 1).

According to that, we generated 10M Poisson randomly distributed events with the expected number of photoelectrons listed above. Besides, the simulation program checked the trigger condition for each event over a trigger threshold range from 1 to 12 photoelectrons. This means that if one event triggered with N photoelectrons, it would also fulfill the topological trigger condition for N-1 photoelectrons and so on.

We'll assume that the electronics will be AC coupled, in such a way that only the fluctuations over the expected average photoelectron population per pixel will go through the electronic readout chain. Given the fact that the average population due to the Cherenkov events is negligible compared to the average population due to NSB, this means in practice that we just subtract to our trigger threshold the expected number of photoelectrons coming from NSB for each photodetector and integration time as listed in Table 1. In some cases, this subtraction leads to negative number of photoelectrons if the number of photoelectrons in a pixels falls below the expected value.

The results of this simulation are summarized in figures 2 and 3. We can see there the trigger rates for 5nsec and 10nsec integration times respectively versus the trigger threshold in photoelectrons. It is worth to notice that in spite of having 10 million of generated diffuse NSB events, the statistics is still too low to achieve a trigger rate of 10 Hz.

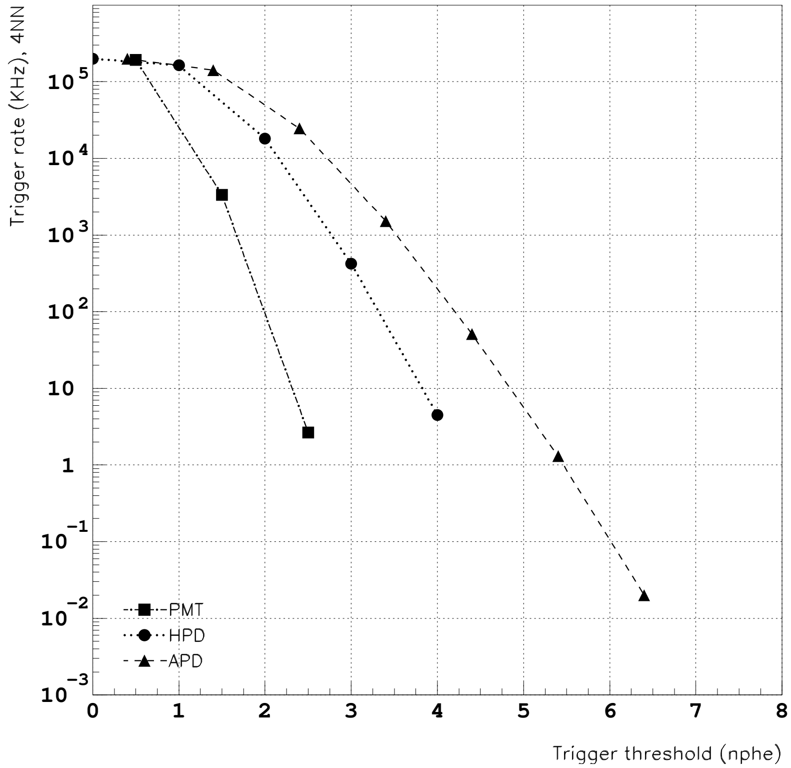

Figure 2: Trigger rate (4NN) vs trigger threshold for 5nsec integration time, DC level subtracted

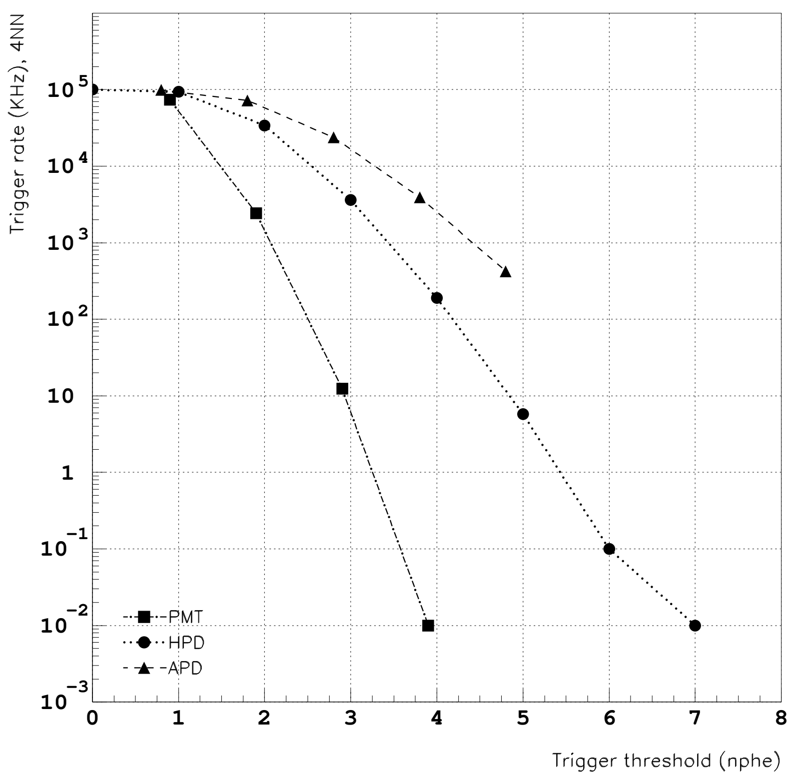

Figure 3: Trigger rate (4NN) vs trigger threshold for 5nsec integration time, DC level subtracted.

4. Calculation of the trigger threshold.

Our aim is to estimate the trigger threshold needed for killing the accidental triggers due to diffuse NSB successfully. For this reason, we set the upper limit of accidental trigger rate at 10% of the total expected trigger rate, that is 10 Hz.

Starting from this point, we computed the trigger threshold for each photodetector, PMT, HPD and APD and integration time, 5 nsec. and 10 nsec. Using two different methods.

4.1 Calculation of the trigger threshold using a polynomial fit.

Keeping in mind the trend of the trigger rate plots given in Figs. 2 and 3, we thought of parameterizing these lines with some function. Since the points with lower trigger rates seem to follow a more or less second order polynomial law in a logarithmic scale, we took the logarithm of the trigger rates and we performed a polynomial fit to this data, see Fig.4.

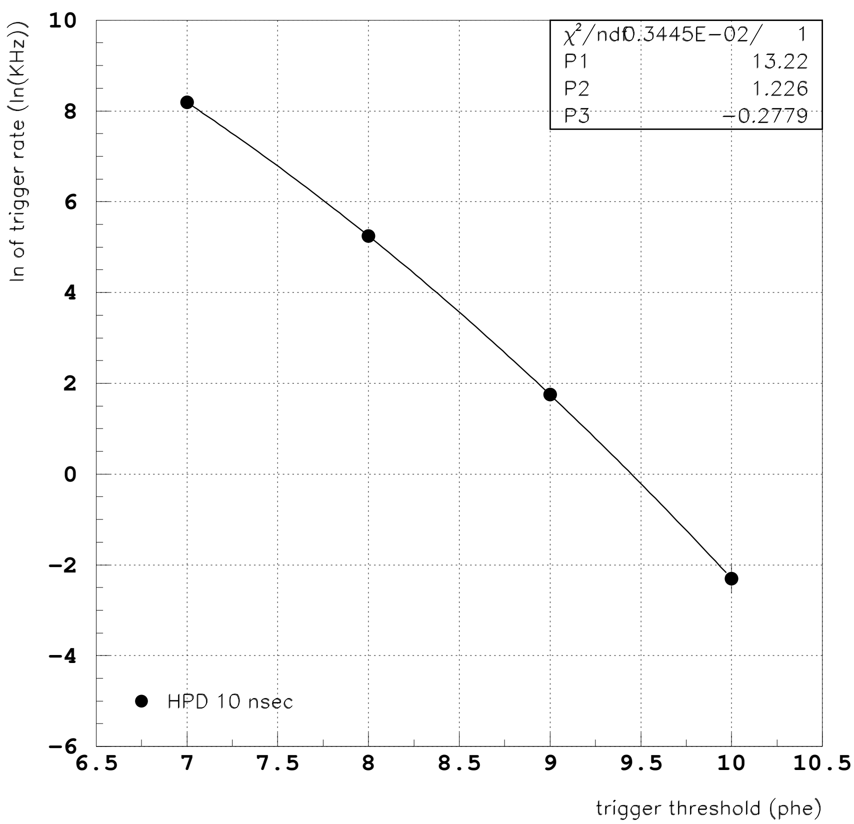

Figure 4: Fit to the logarithm of the trigger rate for HPD and 10nsec integration time.

The results of these calculations are listed in Table 2.

Photo-Detector	Integration time (nsec)	<number of photoelectrons>	Trigger threshold[1] (phe)
PMT	5	0.5	3.08
HPD	5	2.0	5.13
APD	5	3.6	6.41
PMT	10	1.1	3.90
HPD	10	4.0	6.54
APD	10	7.2	8.15

Table 2: Trigger thresholds for 10 Hz of diffuse NSB events using a polynomial fit, DC level subtracted.

But, in spite of obtaining quite good fits, we do not know of any simple theoretical argument to expect this kind of function to fit our trigger rate data. Therefore, to assess on the validity of the obtained results we've also explored another approach in order to compare the two sets of results.

4.2 Calculation of the trigger threshold using the combinatorial factor.

Let's consider the probability P_T of having 4 close-packed pixels above a certain trigger threshold. We obtain P_T by calculating the ratio of triggered events fulfilling the topological trigger condition with a certain trigger threshold and the total number of simulated diffuse NSB events, that is 10^7 events.

This probability can be expanded in terms of the probability of having 1 pixel above a certain photoelectron threshold, P_1:

$$P_T = C_4 \cdot P_1^4 + ... \qquad (4)$$

C_4 is the combinatorial factor and it depends on the topological trigger condition.

If the P_1 is very small, as it is in our case, we can truncate this series and only take the first term. We rename P_1^4 as P_4. . The next step was to plot P_T /P_4 vs P_1 for the 3 types of photodetectors and for both integration times, 5 nsec and 10 nsec (see Fig. 5).

[1] We don't include the systematic and statistical errors because there were very small, less than 10%.

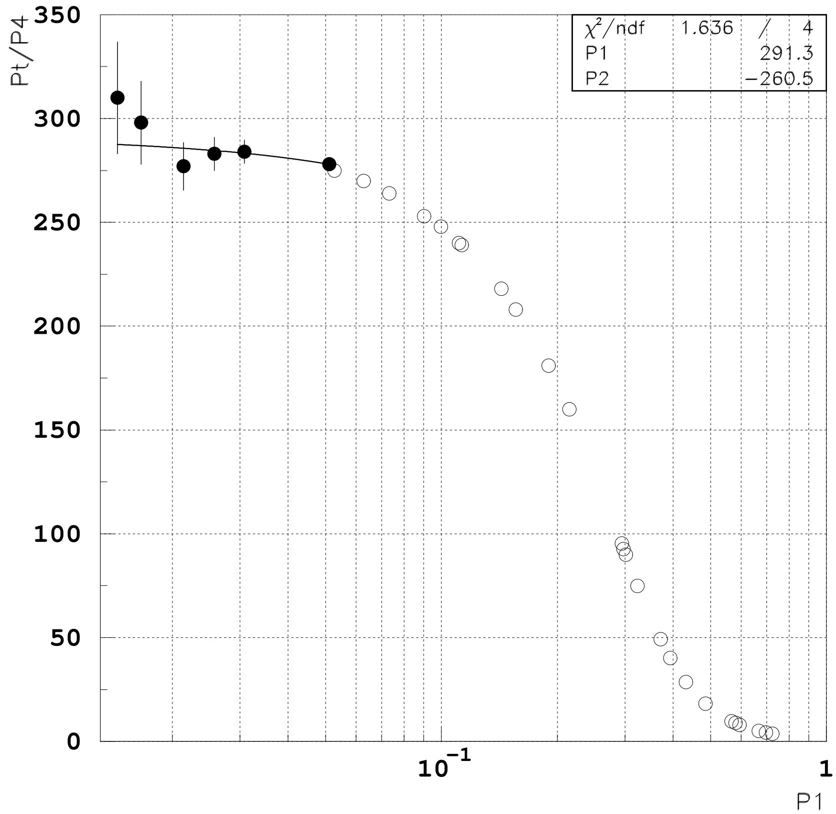

Figure 5: Pt/P4 versus P1 for PMT, HPD, APD and both 5nsec and 10nsec integration times.

Notice that the combinatorial factor doesn't depend on the photodetector used nor on the integration time. Besides, we took the points with small probability P_1, namely $P_1 < 6 \cdot 10^{-2}$, we fitted the data with a linear regression, as we can see in Fig. 5. That is:

$$\frac{P_T}{P_4} = C_4 + C \cdot \vartheta(P_1) \qquad (5)$$

As a result, we could obtain the combinatorial factor, C_4:

$$C_4 = 291.3 \pm 8.9 \qquad (6)$$

Next step was to determinate the trigger threshold assuming only 10 Hz of accidental trigger rate due to diffuse NSB. Since C_4 is the ratio P_T / P_4 and P_T is the trigger rate multiplied by the integration time, we can compute P_4 and P_1 for every integration time. We obtained the following values:

Integration time (nsec)	P_1
5	3.620
10	4.304

Table 3: P_1 values for 5 nsec and 10 nsec integration times.

It's worth to remember that P_1 is given by the cumulative Poisson probability function, that is, the probability that a given number of Poisson random distributed events will be between k and infinity inclusive, if the expected mean number is x:

$$P_1 = P_x(\geq k) = \frac{1}{\Gamma(k)} \int_0^x e^{-t} \cdot t^{k-1} \cdot dt \qquad (7)$$

We take the continuous cumulative Poisson probability function instead of the discrete Poisson probability function, namely:

$$P_1 = P_x(\geq k) = 1 - \sum_{n=0}^{k-1} \frac{e^{-x} \cdot x^n}{n!} \qquad (8)$$

This is because for our numerical calculations the continuous function was easier to handle. However, we make some discrete tests by calculating the Poisson probability function of some trigger thresholds by both formulae and the results that we obtained were very similar, with less than 10% difference.

With these results we were able to invert P_1 and extract the trigger threshold for each photodetector and integration time by numerical methods. We list the results of this second method in Table 4.

Photo-Detector	**Integration time (nsec)**	**<number of photoelectrons>**	**Trigger threshold [1](phe)**
PMT	5	0.5	3.17
HPD	5	2.0	5.16
APD	5	3.6	6.50
PMT	10	1.1	4.04
HPD	10	4.0	6.61
APD	10	7.2	8.44

Table 4: Trigger thresholds for 10 Hz of diffuse NSB events using the combinatorial factor method, DC level subtracted.

[1] We don't put the errors for the same reason than in table 2.

4.3 Comparison of results obtained by both methods.

We can see the trigger threshold values obtained by the two different methods are in agreement in a 5% level, in spite of the ad-hoc use of the polynomial fit method. Notice that for APD 10 nsec integration time, the difference is larger. The polynomial fit method is not so reliable in this case since for achieving an accidental trigger rate of 10 Hz we were forced to do a big extrapolation from our fitted data, as you can see in Fig. 3.

We list in Table 5 the results of both methods.

Photo-Detector	Integration time (nsec)	<number of photoelectrons>	Trigger threshold (phe) (polynomial fit)	Trigger threshold (phe) (combinatorial factor)
PMT	5	0.5	3.08	3.17
HPD	5	2.0	5.13	5.16
APD	5	3.6	6.41	6.50
PMT	10	1.1	3.90	4.04
HPD	10	4.0	6.54	6.61
APD	10	7.2	8.15	8.44

Table 5: Trigger thresholds for 10 Hz of diffuse NSB obtained by the polynomial fit and combinatorial factor methods, DC level subtracted.

We can say that there're no significant differences between both results. We must keep in mind that at hardware level, the actual precision at which the trigger level can be set is likely much worse than the discrepancies we get comparing both results.

5. Rejection of diffuse NSB events using image parameters.

We can also reject diffuse NSB events by performing an off-line or on-line (in a second level trigger, for example) second-moment analysis of the image in the camera plane. We know that the gamma images have an elliptical shape, pointing towards the camera center (provided our telescope is pointing towards the gamma ray source). On the other hand, the diffuse NSB images spread over the whole camera plane.

These parameters, known as *Hillas' parameters* [5], determine the position, orientation, shape and brightness of the image in the camera. For example, Width and Length parameters are the rms spread of light along the minor and major axes of the image, respectively. Distance is the angular distance from the image centroid to the center of the Field of View (FoV). The Alpha parameter is the angle between the major axis of the image and the line connecting the image centroid and the center of the FoV. Size is the total number of photoelectrons in the image and

Conc is the concentration of photons in the image (ratio between the sum of the two pixels with a major number of photoelectrons and the total number of photoelectrons contained in the image). There are still two parameters left: Azwidth and Miss. They are obtained by making combinations of other parameters.

We made an analysis of the following parameters: Length, Width, Alpha and Conc, since these are the most discriminating ones. The first two parameters are larger than 1^0 for diffuse NSB events. On the other hand, and for gamma events, these parameters rarely exceed this value. Besides, the Alpha parameter for diffuse NSB events is rather uniform and for gamma events this parameter is quite low, let's say, below 30^0. But the most discriminating one appears to be the Conc parameter. We noticed that the Conc parameter for diffuse NSB events is an order of magnitude lower than for gamma events.

For our studies we generated 300 gamma showers of 10 GeV and 50 m impact parameter and 300 diffuse NSB events. The photodetector used or the simulation was the HPD. In Fig. 6 we can see the results.

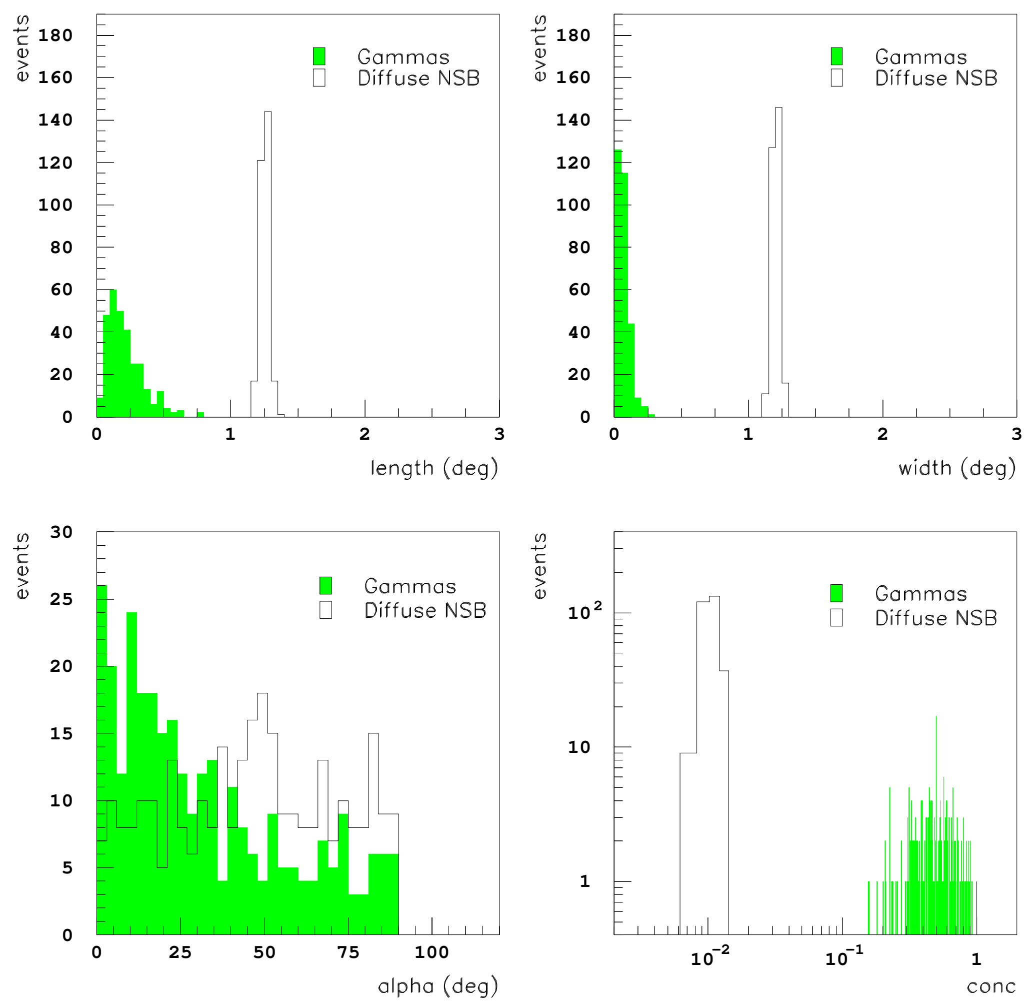

Figure 6: Length, Width, Alpha and Conc image parameters for 10 GeV and 50 m impact parameter gamma events and diffuse NSB events.

We can also use the 4 parameters left: Dist, Azwidth, Miss and Size. However, Dist parameter is less discriminating than Length and Width parameters, as you can see in Fig. 6. Azimuth Width and Miss parameters are combinations of other parameters (Alpha and Width for the first one and Alpha and Dist for the second one). Besides, the Size parameter doesn't help us to distinguish *small* showers (the less energetic ones, for example, 10 GeV) from diffuse NSB events, since the amount of photoelectrons in the image is nearly the same in both cases.

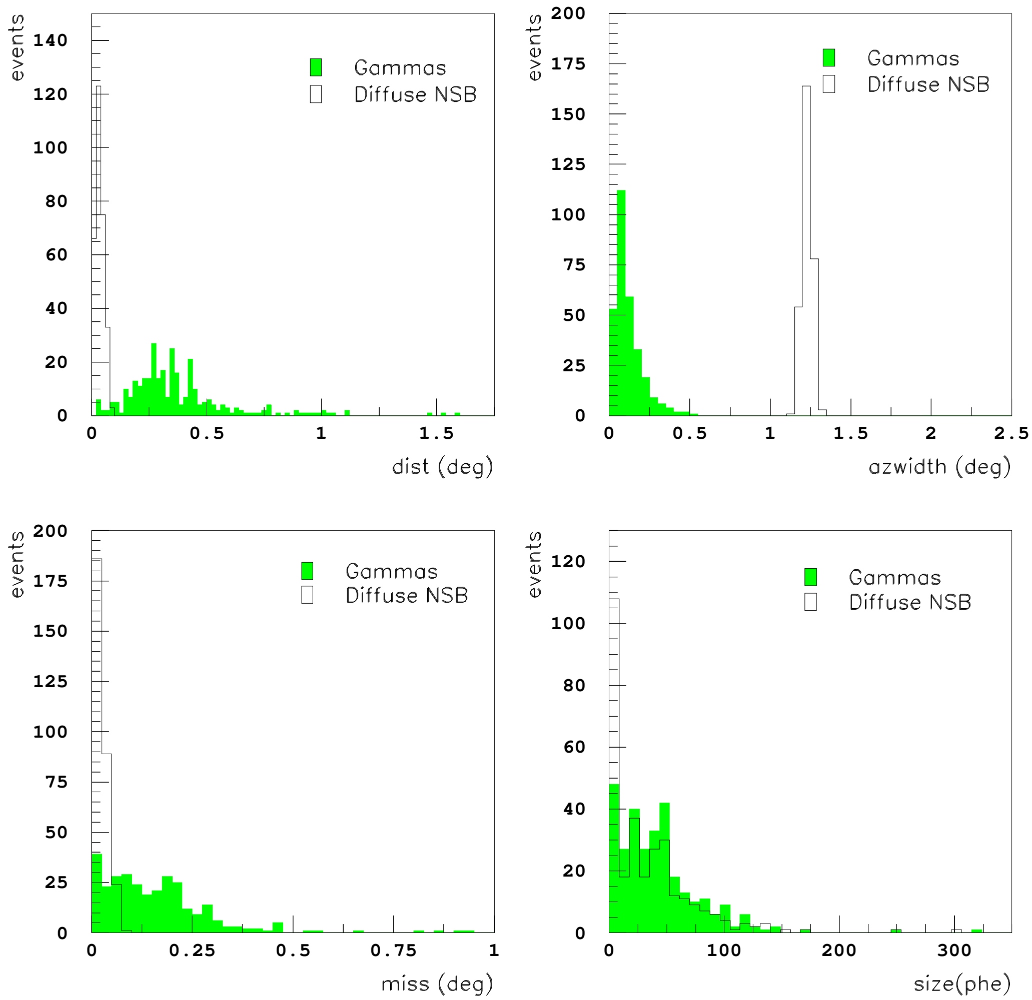

Figure 7: Dist, Azwidth, Miss and Size image parameters for 10 GeV and 50 m impact parameter gamma events and diffuse NSB events.

6. Calculation of the trigger threshold taking into account the electronic noise.

6.1 Parameterization used for the noisy events generation.

Finally, we generated 10 million LONS events, for each photodetector and integration time, including the electronic noise. For the APD case we used McIntyre's theory, see reference [6], [7] and [8], for computing the ENF and for the Monte Carlo generation of the actual APD gain in each cell in each event. The parameters used for the simulation are summarized in Table 6.

Photo-Detector	**Quantum Efficiency**[1]	**Equivalent noise charge**[2]	**Gain**	**Xkeff** [3]	**Excess noise factor**
PMT	0.12	1000	10000	-	1.2
HPD	0.45	1000	10000	-	1.05
APD	0.80	500	3000	$7.2 \cdot 10^{-4}$	McIntyre's[4] ~4.15

Table 6: Noise parameterization used in the simulation.

6.2 Results using both polynomial fit and combinatorial factor methods.

Besides, we computed the trigger thresholds needed for having 10 Hz of accidental trigger rate due to diffuse NSB with electronic noise added using the two methods explained in 4.1 and 4.2. We obtained similar results for the HPD and PMT cases but for APD the trigger threshold doubled its value. In other words, for the APD case, the electronic noise is an important constraint.

The results obtained by both methods were different. That's because, in the way we were using it, the combinatorial factor method doesn't take into account the electronic noise distribution. That is, P_1, which is the Poisson probability that one pixel triggers above a certain threshold, doesn't have any noise consideration since the expected number of photoelectrons due to diffuse NSB doesn't change. These effects are bigger in the APD case since the electronic noise plays an important role in this case. To summarize: the use in this case of the combinatorial factor method requires the detailed parameterization of the single pixel photon probability distribution, which complicates quite a bit the procedure. Because of this fact and, in addition, the good agreement between both procedures observed in the previous case, we've decided to rely now on the polynomial fit alone.

The results of polynomial fit method are given in Table 7. We can compare these results with the ones given in Table 5.

---

[1] Average quantum efficiency for the 300-600 nm wavelength range

[2] This equivalent noise charge is not amplified

[3] Effective ratio between hole and electron ionization coefficients

[4] The ENF in this case is simulated using McIntyre's probability distribution function

Photo-Detector	Integration time (nsec)	<number of photoelectrons>	Trigger threshold (phe) (polynomial fit)
PMT	5	0.5	3.30
HPD	5	2.0	5.00
APD	5	3.6	**17.79**
PMT	10	1.1	4.12
HPD	10	4.0	6.26
APD	10	7.2	**16.77**

Table 7: Trigger thresholds for 10 Hz of diffuse NSB (electronic noise added) obtained by the polynomial fit method. DC level subtracted.

It's worth mentioning that the distributions of the number of photoelectrons for a given photosensor with and without electronic noise implementation are rather different. By including the electronic noise to our diffuse NSB events the distribution of the number of photoelectrons inside each pixel becomes wider. Furthermore, this leads to the fact that the trigger rates without noise implementation can be higher than the trigger rates adding electronic noise, as we'll see later.

The key of this behavior is shown in Figure 8. We simulated a photosensor with 15 expected number of photoelectrons, gain 10^4, excess noise factor 3 and equivalent noise charge 1000. Here we plot the number of photoelectrons distribution for each pixel, with and without noise implementation. When the trigger threshold is, for example, around 2 photoelectrons, the trigger rate for the events without electronic noise will be higher than the trigger rate for the events without electronic noise implementation. Let's remind that the trigger rate is proportional to the probability of triggering, that is, the normalized area below the distribution curve to the right of the 2 photoelectron point. On the other hand, when the trigger threshold is, let's say, 26 photoelectrons, the trigger rate is higher for the events with electronic noise implementation.

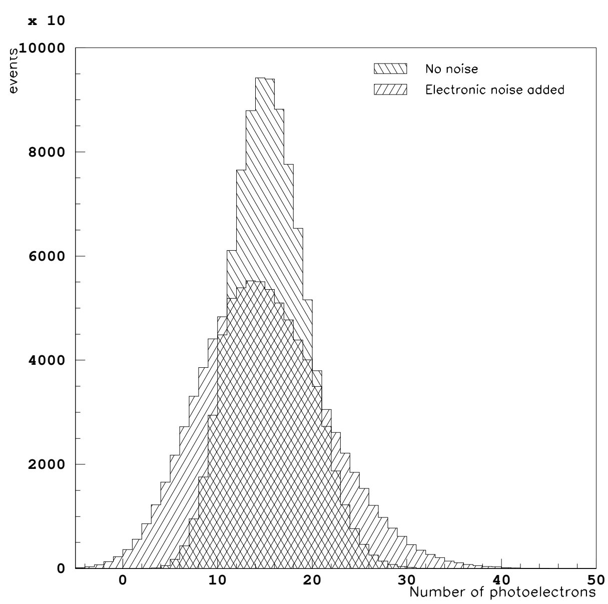

Figure 8: Number of photoelectrons distribution with and without electronic noise implementation for a 'test' photodetector

Besides, in figure 9 we plot the distribution of the number of photoelectrons for pixel for the cases being considered in this study. We took 5nsec integration time and the 3 photosensors used: PMT, HPD and APD. Notice the single photoelectron resolution in the HPD case.

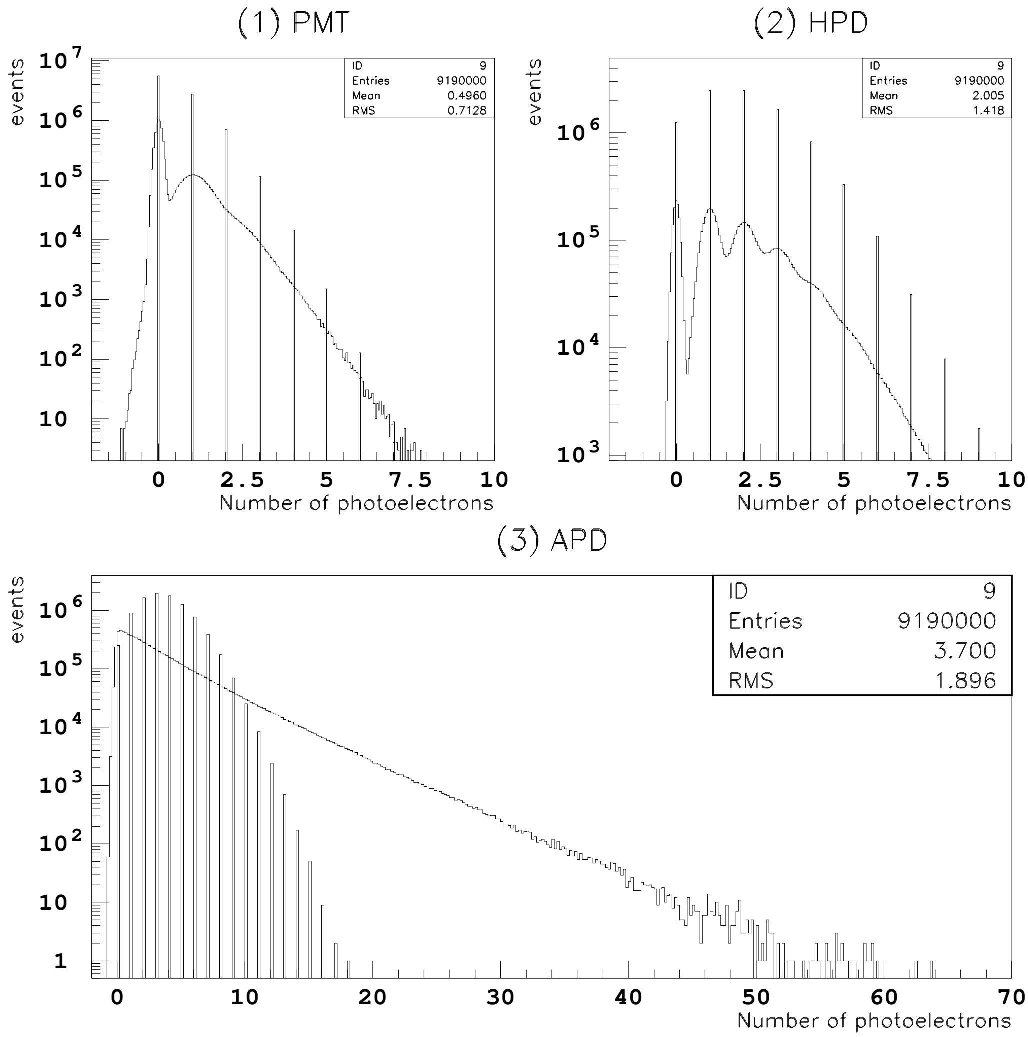

Figure 9: Number of photoelectron distribution in a pixel for 5nsec integration time, PMT, HPD and APD cases. The continuous distribution corresponds to the diffuse NSB events with electronic noise added.

6.3 Comparison: NSB with or without electronic noise.

As we said before, we can conclude that the electronic noise addition mainly affects the trigger architecture for the APD case, since the ENF in these devices is bigger due to the avalanche process amplification. We plot in Figs. 10 and 11 the trigger rate versus the trigger threshold for 5nsec and 10nsec integration times respectively. The dashed lines correspond to the events with electronic noise included and the solid lines correspond to the events without implementing the electronic noise.

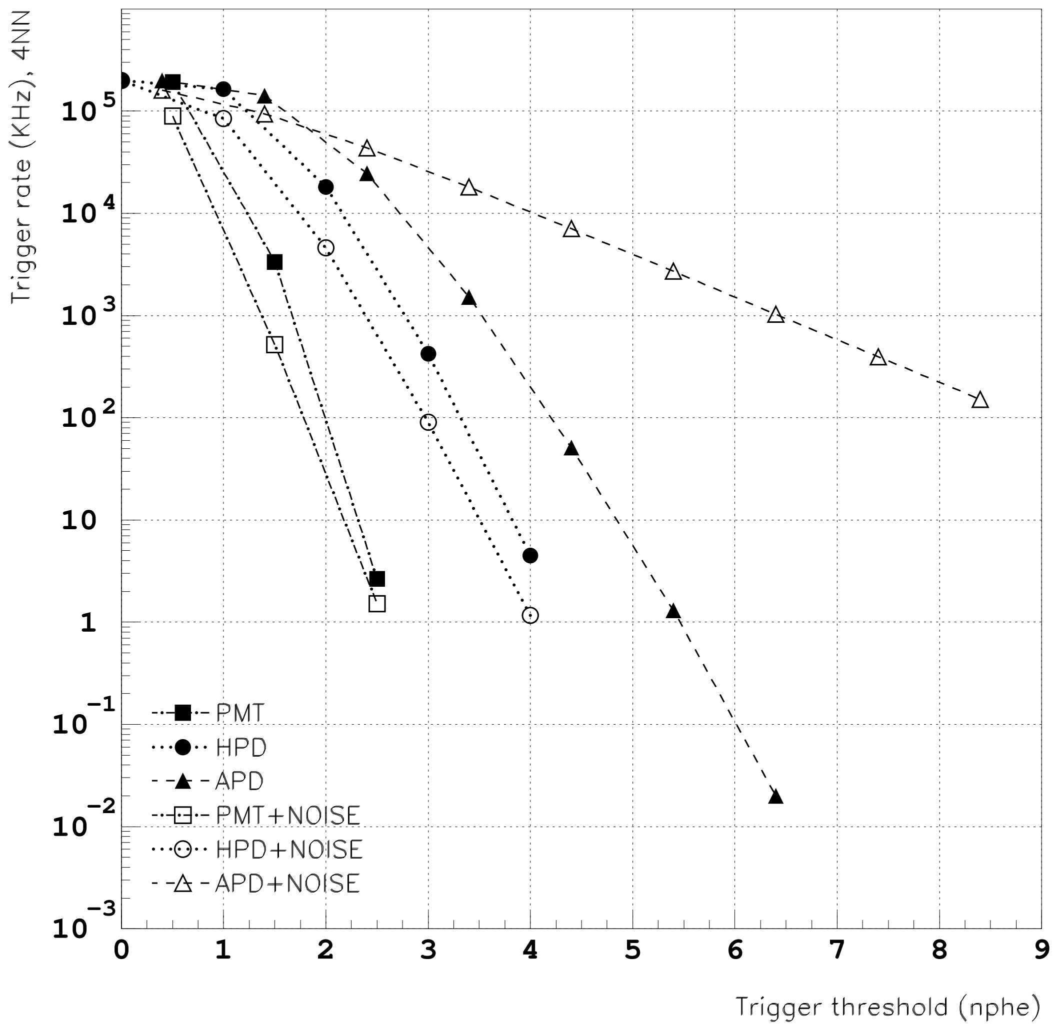

Figure 10: Trigger rate (4NN) vs trigger threshold for diffuse NSB events, 5 nsec integration time, with and without electronic noise. DC level subtracted.

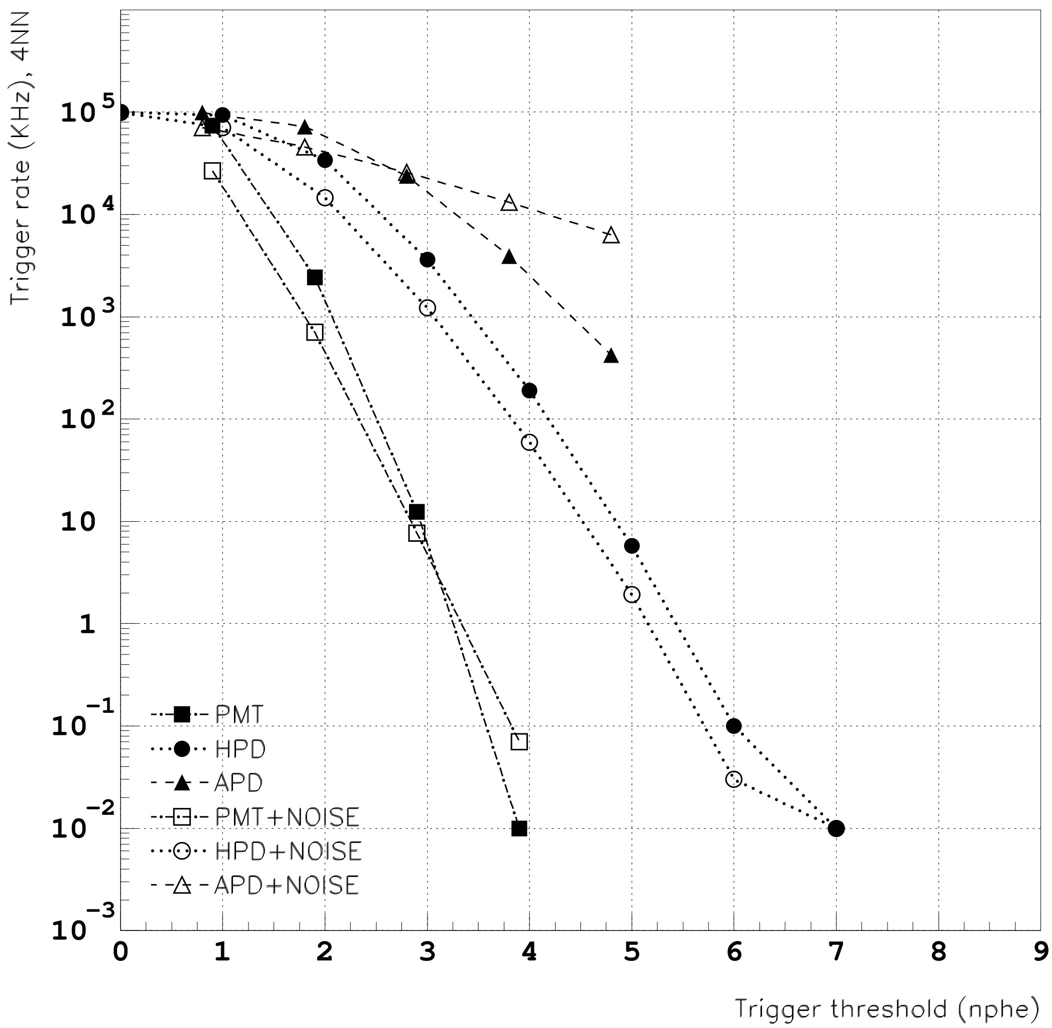

Figure 11: Trigger rate vs trigger threshold for diffuse NSB events, 10 nsec integration time, with and without electronic noise. DC level subtracted.

7. Conclusions.

We have studied the influence of the diffuse component of the Night Sky Background in the photosensor choice for the next generation of Cherenkov telescopes which aim to reduce as much as possible the trigger threshold. Simulations taking into account different noise sources and a realistic trigger scheme have been performed to determine the expected trigger rate as a function of the trigger threshold.

Our results show that in realistic conditions, if one aims for Night Sky Background trigger rates below 10 Hz (about 1/10 of the expected signal for low threshold) the use of high quantum efficiency photosensors such ad HPDs and APDs will be possible for trigger thresholds above 5 and 18 photoelectrons respectively if the system response time is of, say, 5 nsec, while it can be set to about 3 photoelectrons for PMTs. The large number for the APD case is mostly due to the effect of its intrinsic amplification noise (Excess Noise Factor).

Nevertheless, we've also shown that the use of simple image analysis parameters, which could be implemented into a second level trigger, may allow a strong further reduction of such background.

8. Acknowledgments.

We thank all the members of the MAGIC collaboration for their help and for providing us with all the necessary information for this study. We are especially indebted to O.C. de Jager, E.Lorenz, R. Mirzoyan, A. Ostankov and O. Blanch for their careful reading of this manuscript and for very valuable comments.

9. References.

[1] MAGIC collaboration, March 1998, 'MAGIC Design Report'

[2] E. Lorenz, M. Martínez, R. Mirzoyan, S. Ostankov, submitted to Nuclear Instr. and Meth., 'Constraints in Using APDs in future Air Cherenkov Telescopes for γ astronomy'

[3] R. Mirzoyan & E. Lorenz, 1994, 'Measurement of the night sky light background at La Palma', Max-Planck-Institut für Physik report MPI-PhE/94-35

[4] J.C. González, et al., 1997, in O. C. de Jager, Towards a Major Atmospheric Cerenkov Detector - V, 'Monte Carlo simulations for the MAGIC Telescope'

[5] A. M. Hillas, Proc. 19th ICRC, La Jolla, 3 (1985) p.445.

[6] McIntyre R. J., IEEE Trans. on Electron Dev., vol.13, nº 1 (1966) p.164.

[7] McIntyre R. J., IEEE Trans. on Electron Dev., vol.19, nº 6 (1972) p.703.

[8] Van Vliet K.M., IEEE Trans. on Electron Dev., vol. 26, nº 5(1979) p 752.

Appendix A

Variations of the trigger region size.

The same studies were performed considering a trigger region of 397 pixels. It is clear that by doubling the FoV in the trigger region the probability of finding a 4 close-packed combination given a certain trigger threshold is much higher in the 127 pixels trigger region case. But when talking about trigger thresholds we have to keep in mind that small variations of the trigger threshold produce big variations of the trigger probability due to fast falling dependency. In Fig. 12 we can see the trigger probability as a function of the trigger threshold (DC level subtracted) for the 2 trigger regions, namely, 397 and 127 pixels. We can distinguish 3 regions:

- Small trigger thresholds.

The probability of triggering is 1 in both cases. We are in a saturation regime and the trigger probability doesn't depend on the trigger region size.

- Intermediate trigger thresholds.

The trigger probabilities of a 397 pixels trigger region is much higher than for the 127 pixels trigger region size. But due to this fast falling dependency on the trigger threshold, these big differences in trigger probability produce small differences in trigger threshold.

- High trigger thresholds.

The probability of triggering is now very small for both cases. In this case, the differences between trigger probabilities get much larger in spite of having small differences in trigger threshold.

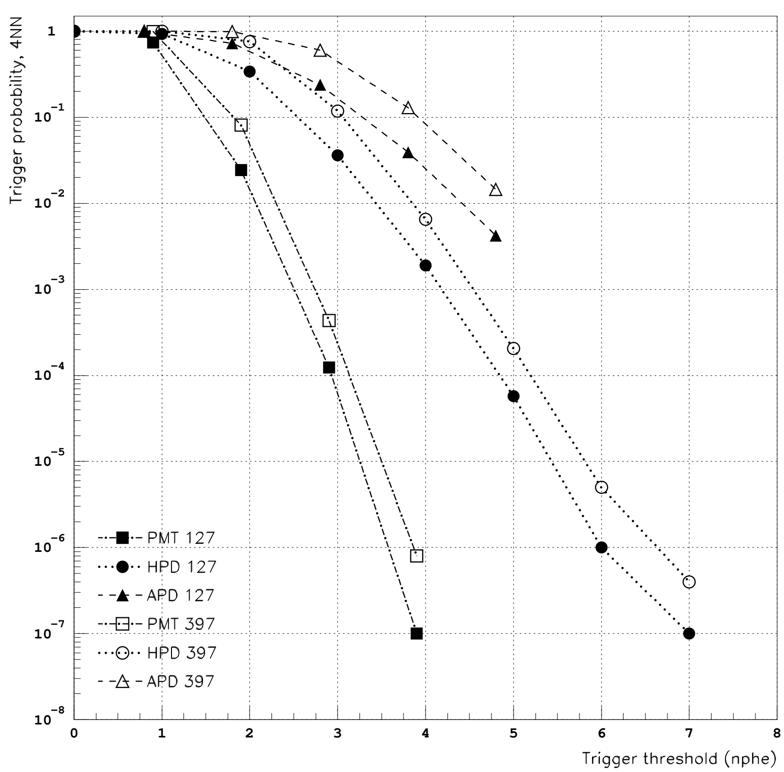

Figure 12: Comparison of trigger probabilities (4NN) as a function of the trigger threshold (DC level subtracted) for 397 and 127 trigger region cameras, 10 nsec

Our conclusion is that doubling the FoV would increase the trigger threshold in less than 1 phe. We summarize the results of our studies, without electronic noise in Table 8. Notice that the DC level is subtracted as well.

			397 Pixels		***127 Pixels***	
Photo-Detector	**Integration time (nsec)**	**<number of photoelectrons>**	**Polynomial fit**	**Combinatorial factor**	**Polynomial fit**	**Combinatorial factor**
PMT	5	0.5	3.14	3.30	3.08	3.17
HPD	5	2.0	5.26	5.37	5.13	5.16
APD	5	3.6	6.86	6.75	6.41	6.50
PMT	10	1.1	4.20	4.22	3.90	4.04
HPD	10	4.0	6.80	6.89	6.54	6.61
APD	10	7.2	8.13	8.78	8.15	8.44

Table 8: Trigger thresholds for 127 and 397 pixels trigger regions obtained by the polynomial fit and combinatorial factor methods. DC level subtracted.